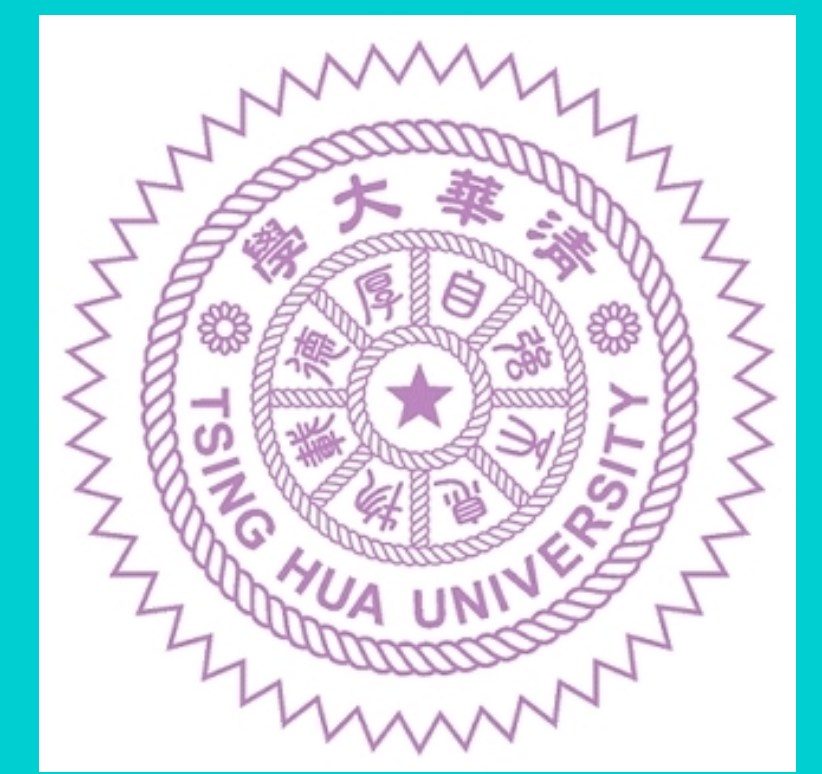


# Type Ia Supernovae Induced by Primordial Black Holes from Dark First-Order Phase Transition

Pin-Jung Chen and Po-Yan Tseng

Department of Physics and CTC, National Tsing Hua University



## Abstract

We applied a novel scenario to impose constraints on the relic abundance  $f_{\text{PBH}}$  of primordial black holes (PBHs) in the mass range  $10^{-14} \leq M_{\text{PBH}}/M_\odot \leq 10^{-11}$  which cannot be probed by microlensing or evaporation methods: When a PBH with the aforementioned mass transits through a white dwarf (WD) made up of carbon and oxygen, Bondi-Hoyle-Lyttleton (BHL) accretion in a reactive medium creates a shock wave, which generates direct detonation ignition in the WD core and then leads to Type Ia supernovae (SNe Ia) whose event rate is to be compared with the observational data. PBHs in the constrained region can be produced by a cosmological first-order phase transition (FOPT) in the dark sector which associates with  $\mathcal{O}(\text{MeV})$  energy scale and thus gives rise to complementary signals of stochastic gravitational waves (GWs) from  $10^{-6}$  Hz to  $10^{-5}$  Hz peak frequency which can be probed by future  $\mu$ Ares GW interferometer.

## PBH formation mechanism

Let  $\phi$  and  $\chi$  be a scalar field and a Dirac particle with  $U(1)$  charge in the dark sector, respectively. Then the simplest Lagrangian density which can realise the PBH formation mechanism illustrated in Fig. 1 is

$$\mathcal{L}_{\text{Dark}} = \frac{1}{2}(\partial_\mu\phi)(\partial^\mu\phi) - V_{\text{eff}}(\phi, T) + \bar{\chi}(i\partial - m_\chi)\chi - g_\chi\phi\bar{\chi}\chi \quad (1)$$

with

$$V_{\text{eff}}(\phi, T) \approx D(T^2 - T_0^2)\phi^2 - (AT + C)\phi^3 + \frac{\lambda(T)}{4}\phi^4. \quad (2)$$

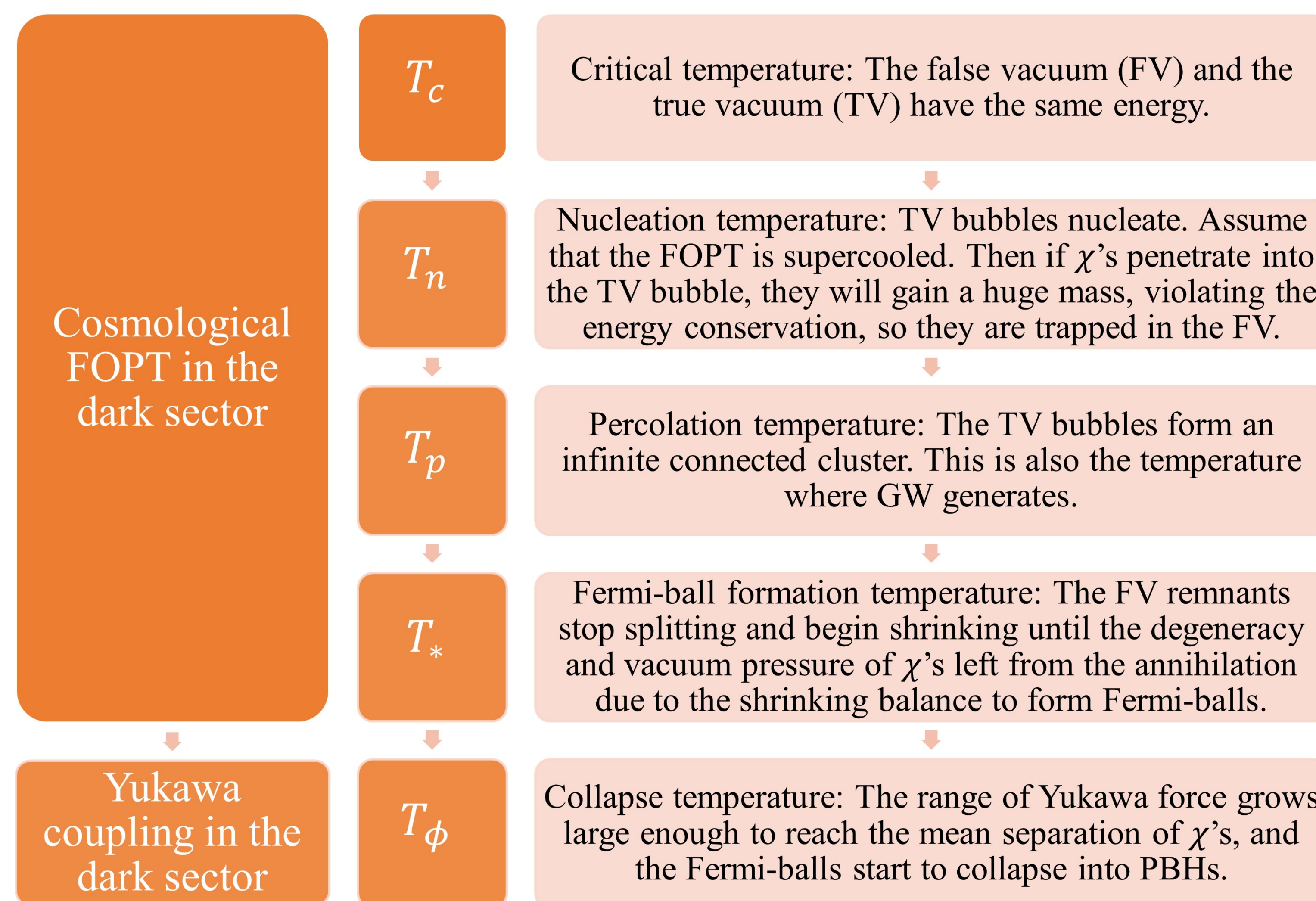


Figure 1. PBH formation mechanism.

## Results

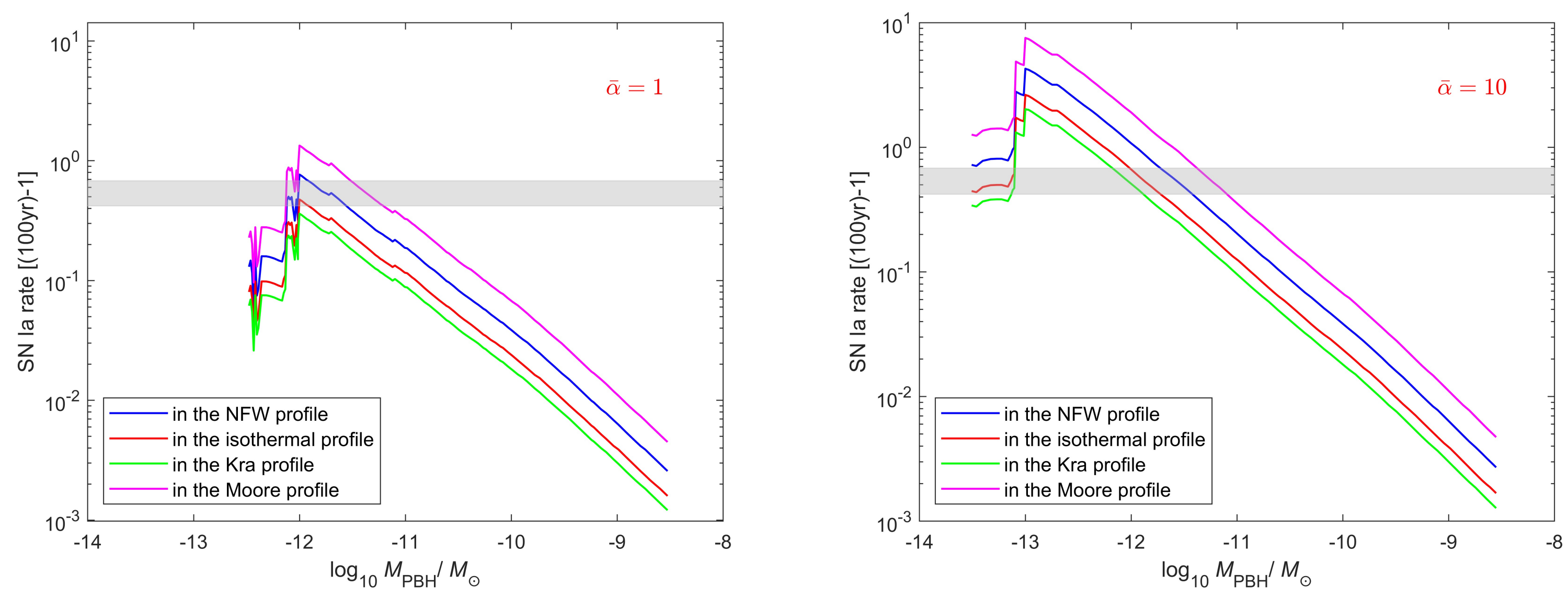


Figure 2. SN Ia event rate induced by PBHs in the NFW, isothermal, Kra and Moore profiles, when  $f_{\text{PBH}}$  is 1 and  $\bar{\alpha}$  is 1 (left) and 10 (right).

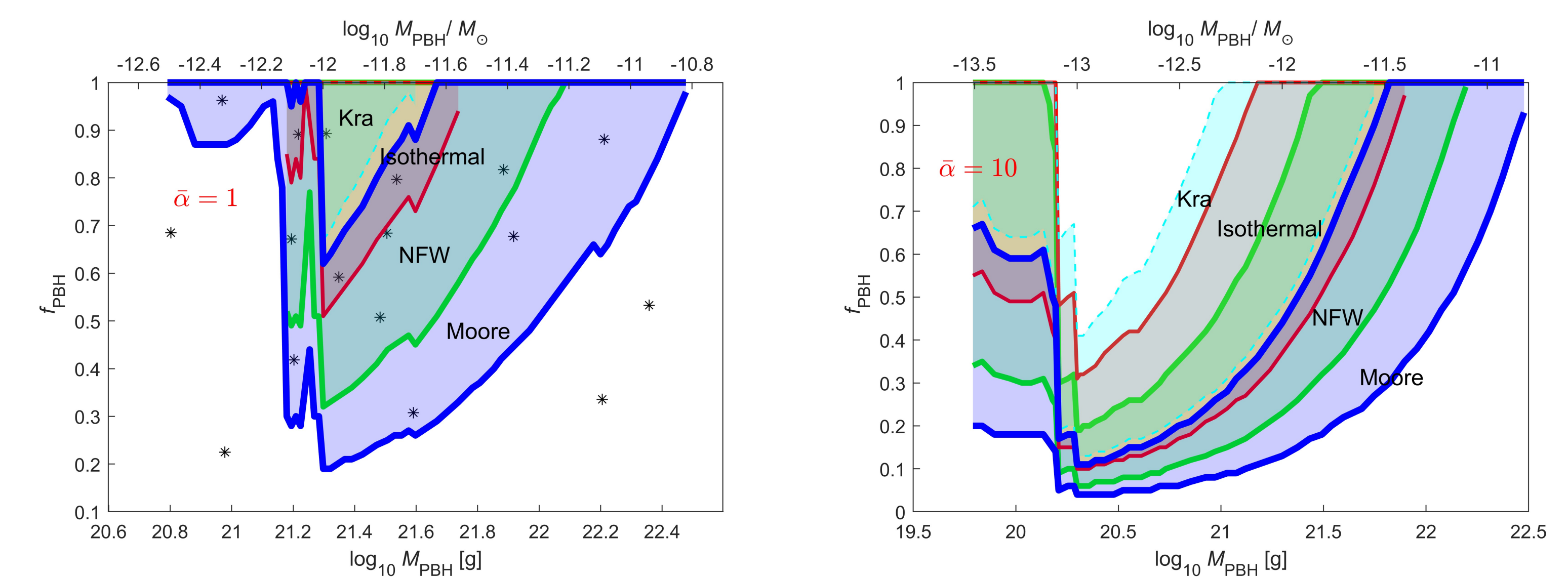


Figure 3. The shaded parameter regions reproduce the observed SN Ia event rate in the NFW (green), isothermal (red), Kra (cyan) and Moore (blue) profiles when  $\bar{\alpha}$  is 1 (left) and 10 (right). The "\*" points within the shaded regions indicate the benchmark points (BPs) belonging to a particular profile in Table 1 and 2; otherwise, they are BP-1 to 4 in Table 2.

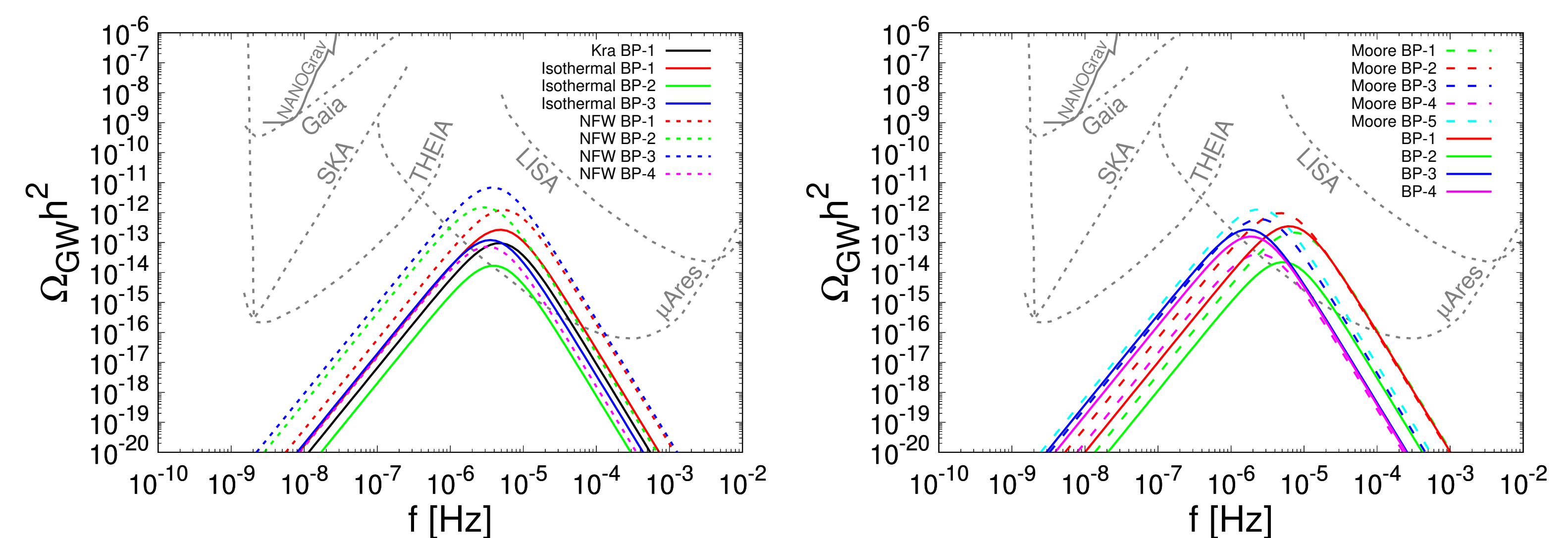


Figure 4. GW power spectra for the BPs in Table 1 (left) and Table 2 (right).

	Kra BP-1	Isothermal BP-1	Isothermal BP-2	Isothermal BP-3	NFW BP-1	NFW BP-2	NFW BP-3	NFW BP-4
$B^{1/4}/\text{MeV}$	4.316	5.477	3.262	2.973	11.72	5.269	9.840	4.433
$\lambda$	0.120	0.104	0.089	0.059	0.057	0.186	0.086	0.123
$D$	0.794	1.243	0.922	1.674	0.629	1.891	1.564	0.434
$\eta_{\text{DM}}$	$2.97 \times 10^{-8}$	$2.73 \times 10^{-8}$	$2.78 \times 10^{-8}$	$3.66 \times 10^{-8}$	$5.89 \times 10^{-9}$	$1.54 \times 10^{-8}$	$9.36 \times 10^{-9}$	$1.87 \times 10^{-8}$
$r_T$	0.506	0.434	0.320	0.379	0.353	0.433	0.361	0.398
$C/\text{MeV}$	0.203	0.240	0.110	0.032	0.343	0.556	0.550	0.353
$g_\chi$	1.520	1.329	1.274	0.807	0.833	1.352	0.822	1.459
$m/B^{1/4}$	0.059	0.020	0.383	1.508	0.936	0.093	0.451	0.699
$M_{\text{PBH}}/M_\odot$	$1.02 \times 10^{-12}$	$8.29 \times 10^{-13}$	$1.12 \times 10^{-12}$	$1.73 \times 10^{-12}$	$7.87 \times 10^{-13}$	$1.53 \times 10^{-12}$	$1.61 \times 10^{-12}$	$3.85 \times 10^{-12}$
$f_{\text{PBH}}$	0.893	0.891	0.592	0.797	0.671	0.508	0.684	0.817
$R(T_*) [\text{GeV}^{-1}]$	$7.23 \times 10^{19}$	$6.13 \times 10^{19}$	$8.18 \times 10^{19}$	$1.61 \times 10^{20}$	$1.84 \times 10^{19}$	$1.15 \times 10^{20}$	$5.00 \times 10^{19}$	$6.43 \times 10^{19}$
$v w$	0.880	0.943	0.930	0.955	0.977	0.969	0.990	0.902
$R_{\text{FB}} [\text{GeV}^{-1}]$	$9.29 \times 10^{17}$	$7.35 \times 10^{17}$	$1.37 \times 10^{18}$	$1.73 \times 10^{18}$	$1.29 \times 10^{17}$	$9.83 \times 10^{17}$	$3.28 \times 10^{17}$	$2.23 \times 10^{17}$
$Q_{\text{FB}}$	$9.50 \times 10^{46}$	$7.05 \times 10^{46}$	$1.40 \times 10^{47}$	$2.17 \times 10^{47}$	$1.89 \times 10^{46}$	$1.32 \times 10^{47}$	$6.37 \times 10^{46}$	$2.38 \times 10^{47}$

Table 1. The BPs in the Kra, isothermal and NFW profiles, which form PBHs after FOPT with  $A = 0.1$  fixed.

	Moore BP-1	Moore BP-2	Moore BP-3	Moore BP-4	Moore BP-5	BP-1	BP-2	BP-3	BP-4
$B^{1/4}/\text{MeV}$	13.27	8.947	3.605	1.214	4.809	9.572	7.175	2.030	3.726
$\lambda$	0.166	0.056	0.184	0.135	0.085	0.153	0.167	0.072	0.199
$D$	0.282	0.430	3.088	3.779	0.991	1.025	0.195	0.756	0.708
$\eta_{\text{DM}}$	$4.93 \times 10^{-9}$	$4.04 \times 10^{-9}$	$1.65 \times 10^{-8}$	$1.48 \times 10^{-7}$	$2.43 \times 10^{-8}$	$8.37 \times 10^{-9}$	$1.94 \times 10^{-9}$	$2.20 \times 10^{-8}$	$1.87 \times 10^{-8}$
$r_T$	0.551	0.421	0.329	0.440	0.367	0.419	0.441	0.421	0.334
$C/\text{MeV}$	1.747	0.159	0.357	0.043	0.247	0.864	1.114	0.051	0.587
$g_\chi$	1.190	0.923	1.445	1.282	1.129	1.156	1.514	1.169	1.837
$m/B^{1/4}$	2.265	1.168	0.027	0.020	0.590	1.400	1.105	0.375	0.012
$M_{\text{PBH}}/M_\odot$	$4.68 \times 10^{-13}$	$8.02 \times 10^{-13}$	$1.96 \times 10^{-12}$	$4.15 \times 10^{-12}$	$8.19 \times 10^{-12}$	$3.19 \times 10^{-13}$	$4.78 \times 10^{-13}$	$8.06 \times 10^{-12}$	$1.15 \times 10^{-11}$
$f_{\text{PBH}}$	0.963	0.418	0.308	0.677	0.881	0.685	0.225	0.335	0.533
$R(T_*) [\text{GeV}^{-1}]$	$9.76 \times 10^{18}$	$2.51 \times 10^{19}$	$2.11 \times 10^{20}$	$8.60 \times 10^{20}$	$1.23 \times 10^{20}$	$2.41 \times 10^{19}$	$1.71 \times 10^{19}$	$3.69 \times 10^{20}$	$1.50 \times 10^{20}$
$v w$	0.850	0.952	0.984	0.925	0.977	0.945	0.818	0.941	0.952
$R_{\text{FB}} [\text{GeV}^{-1}]$	$5.87 \times 10^{16}$	$1.52 \times 10^{17}$	$2.06 \times 10^{18}$	$1.89 \times 10^{19}$	$1.31 \times 10^{18}$	$1.70 \times 10^{17}$	$1.14 \times 10^{17}$	$4.21 \times 10^{18}$	$1.95 \times 10^{18}$
$Q_{\text{FB}}$	$6.71 \times 10^{45}$	$2.14 \times 10^{46}$	$2.90 \times 10^{47}$	$2.50 \times 10^{48}$	$6.27 \times 10^{47}$	$1.07 \times 10^{46}$	$1.12 \times 10^{46}$	$1.45 \times 10^{48}$	$1.08 \times 10^{48}$

Table 2. The BPs in the Moore profile and outside all the profiles, which form PBHs after FOPT with  $A = 0.1$  fixed.

## References

- [1] P. J. Chen and P. Y. Tseng, JHEAp **39**, 106-113 (2023) doi:10.1016/j.jheap.2023.07.002 [arXiv:2305.14399 [astro-ph.HE]].
- [2] H. Steigerwald and E. Tejeda, Phys. Rev. Lett. **127**, no. 1, 011101 (2021) doi:10.1103/PhysRevLett.127.011101 [arXiv:2104.07066 [astro-ph.HE]].
- [3] K. Kawana and K. P. Xie, Phys. Lett. B **824**, 136791 (2022) doi:10.1016/j.physletb.2021.136791 [arXiv:2106.00111 [astro-ph.CO]].
- [4] J. P. Hong, S. Jung and K. P. Xie, Phys. Rev. D **102**, no. 7, 075028 (2020) doi:10.1103/PhysRevD.102.075028 [arXiv:2008.04430 [hep-ph]].
- [5] D. Marfatia and P. Y. Tseng, JHEP **11**, 068 (2021) doi:10.1007/JHEP11(2021)068 [arXiv:2107.00859 [hep-ph]].